American Control Conference (ACC'06), Minneapolis, Minnesota USA, June 14-16, 2006

# A Unified Control Concept for Autonomous Underwater Vehicles

Morten Breivik*,[1]
*Centre for Ships and Ocean Structures (CESOS)
Norwegian University of Science and Technology (NTNU)
NO-7491 Trondheim, Norway
E-mail: morten.breivik@ieee.org

Thor I. Fossen*,†
†Department of Engineering Cybernetics (ITK)
Norwegian University of Science and Technology (NTNU)
NO-7491 Trondheim, Norway
E-mail: fossen@ieee.org

*Abstract*— **This paper addresses the problem of creating a controller structure for the automatic control of autonomous underwater vehicles (AUVs) through their entire non-zero speed regimes, without resorting to switching between structurally different controllers. A single controller structure is proposed for the purpose, whose core is a nonlinear, model-based velocity and attitude controller that relies on a key guidance-based path following concept necessary to ensure geometric path convergence. The scheme renders all regular paths feasible, and ensures that an AUV which is fully actuated at low speeds, but becomes underactuated at high speeds, is able to converge to and follow a desired geometric path independent of the current vehicle speed.**

## I. Introduction

The number of autonomous underwater vehicles (AUVs) roaming the seas of the world is rapidly increasing, mainly due to tasks originating from various commercial, military and scientific needs. In this context, the ability for the AUVs to maneuver accurately and safely both in space and time is fundamental. Hence, it is essential to be able to automatically control the vehicles through all the stages from low-speed positioning to high-speed maneuvering.

Traditionally, at least for marine surface vessels, such a problem has been solved by constructing dedicated controllers for each distinct part of the speed envelope. For low-speed applications it is assumed that the vessel in question is fully actuated for the purpose, while underactuation is assumed for high speeds. This has led to the development of structurally different controllers, where the desired functionality is obtained by using a supervisor to intelligently switch between the different designs. However, it would be very desirable to devise a single controller structure, without resorting to heuristics and hybrid switching, to cover the entire non-zero speed envelope of an AUV. This could lead to reduced complexity of implementation, easier code verification and maintenance procedures, and possibly increased safety of operation. In practice, the only relevant type of AUVs to consider are the ones which become underactuated in the sway, heave and roll DOFs.

[1]This work was supported by the Research Council of Norway through the Centre for Ships and Ocean Structures at NTNU.

### A. Previous Work

The literature concerning the desired control topic for AUVs is virtually non-existent. A low-speed positioning application can be found in [1], while [2] treats high-speed maneuvering. However, no work seems to deal with operation throughout the non-zero speed regime. Still, some applications are reported for marine surface vessels. A hybrid switching design involving a dynamic positioning controller for low speeds and a track-keeping controller for high speeds is reported in [3], while [4] proposes a unified design.

### B. Main Contribution

This concept paper proposes a single controller structure capable of controlling an AUV operating in a 3D ocean space through its entire non-zero speed envelope. The core of the structure consists of a nonlinear, model-based velocity and attitude controller which relies on a key guidance-based path following concept necessary to guarantee geometric path convergence. The scheme is a natural extension of the path following approach in [5] where the individual designs for the fully actuated and underactuated cases have been fusioned into one, seamless design without any heuristics involved. The paper contains a lucid exposition of the proposed approach, which is physically intuitive.

## II. Problem Statement

The primary objective in guidance-based path following is to ensure that a vehicle converges to and follows a desired geometric path, without any temporal requirements. The secondary objective is to ensure that the vehicle complies with a desired dynamic behavior. By using the convenient task classification scheme in [6], the guidance-based path following problem can thus be expressed by the following two task objectives:

**Geometric Task:** Make the position of the vehicle converge to and follow a desired geometric path.

**Dynamic Task:** Make the speed of the vehicle converge to and track a desired speed assignment.

When both task objectives for some reason cannot be met simultaneously, the geometric one has precedence over the dynamic one.

## III. Ideal Guidance Concept

The content of this section is taken from [7]. We will consistently employ the notion of an *ideal particle*, which basically is a spatial position variable without dynamics (i.e. a kinematic particle), free to move anywhere in 3D space. We will also utilize the notion of a *path particle*, which is a spatial position variable restricted to move along the geometric path it is associated with.

### A. Assumptions

The following assumptions are made:

**A.1** The desired geometric path is regularly parametrized.
**A.2** The speed of the ideal particle is lower-bounded.
**A.3** The guidance variables are positive and upper-bounded.

### B. Ideal Guidance Laws

Denote the position and velocity vectors of the ideal particle in the INERTIAL frame (**I**) by $\mathbf{p} = [x, y, z]^\top \in \mathbb{R}^3$ and $\dot{\mathbf{p}} = [\dot{x}, \dot{y}, \dot{z}]^\top \in \mathbb{R}^3$, respectively. Denote the size of the velocity vector by $U = |\dot{\mathbf{p}}|_2 = (\dot{\mathbf{p}}^\top \dot{\mathbf{p}})^{\frac{1}{2}}$ (the speed), and let the orientation be characterized by the two angular variables:

$$\chi = \arctan\left(\frac{\dot{y}}{\dot{x}}\right), \tag{1}$$

which is denoted the azimuth angle, and:

$$\upsilon = \arctan\left(\frac{-\dot{z}}{\sqrt{\dot{x}^2 + \dot{y}^2}}\right), \tag{2}$$

denoted the elevation angle. Since it is assumed that for an ideal particle $U$, $\chi$ and $\upsilon$ can attain any desirable value instantaneously, rewrite them as $U_\mathrm{d}$, $\chi_\mathrm{d}$ and $\upsilon_\mathrm{d}$.

Consider a geometric path continuously parametrized by a scalar variable $\varpi \in \mathbb{R}$, and denote the inertial position of its path particle as $\mathbf{p}_\mathrm{p}(\varpi) \in \mathbb{R}^3$. Consequently, the geometric path can be expressed by the set:

$$\mathcal{P} = \left\{\mathbf{p} \in \mathbb{R}^3 \mid \mathbf{p} = \mathbf{p}_\mathrm{p}(\varpi)\ \forall \varpi \in \mathbb{R}\right\}, \tag{3}$$

where $\mathcal{P} \subset \mathbb{R}^3$.

For a given $\varpi$, define a local reference frame at $\mathbf{p}_\mathrm{p}(\varpi)$ and name it the PATH frame (**P**). To arrive at **P**, we need to perform two consecutive elementary rotations (when using the concept of Euler angles). The first is to positively rotate the INERTIAL frame (**I**) an angle:

$$\chi_\mathrm{p}(\varpi) = \arctan\left(\frac{y'_\mathrm{p}(\varpi)}{x'_\mathrm{p}(\varpi)}\right) \tag{4}$$

about its $z$-axis, where the notation $x'_\mathrm{p}(\varpi) = \frac{\mathrm{d}x_\mathrm{p}}{\mathrm{d}\varpi}(\varpi)$ has been utilized. This rotation can be represented by the rotation matrix:

$$\mathbf{R}_{\mathrm{p,z}}(\chi_\mathrm{p}) = \begin{bmatrix} \cos\chi_\mathrm{p} & -\sin\chi_\mathrm{p} & 0 \\ \sin\chi_\mathrm{p} & \cos\chi_\mathrm{p} & 0 \\ 0 & 0 & 1 \end{bmatrix}, \tag{5}$$

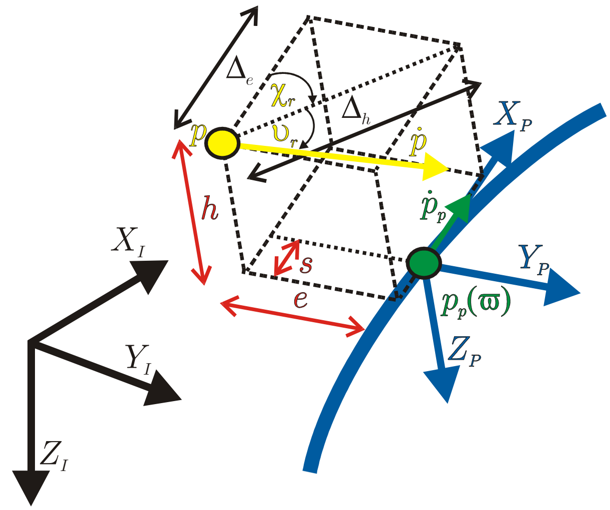


Fig. 1. The geometric relationship between all the relevant parameters and variables utilized in the proposed guidance-based path following scheme in 3D, $\mu = 1$.

where $\mathbf{R}_{\mathrm{p,z}} \in SO(3)$. The second rotation is performed by positively rotating the resulting intermediate frame an angle:

$$\upsilon_\mathrm{p}(\varpi) = \arctan\left(\frac{-z'_\mathrm{p}(\varpi)}{\sqrt{x'_\mathrm{p}(\varpi)^2 + y'_\mathrm{p}(\varpi)^2}}\right) \tag{6}$$

about its $y$-axis. This rotation can be represented by the rotation matrix:

$$\mathbf{R}_{\mathrm{p,y}}(\upsilon_\mathrm{p}) = \begin{bmatrix} \cos\upsilon_\mathrm{p} & 0 & \sin\upsilon_\mathrm{p} \\ 0 & 1 & 0 \\ -\sin\upsilon_\mathrm{p} & 0 & \cos\upsilon_\mathrm{p} \end{bmatrix}, \tag{7}$$

where $\mathbf{R}_{\mathrm{p,y}} \in SO(3)$. Hence, the full rotation can be represented by the rotation matrix:

$$\mathbf{R}_\mathrm{p} = \mathbf{R}_{\mathrm{p,z}}(\chi_\mathrm{p})\mathbf{R}_{\mathrm{p,y}}(\upsilon_\mathrm{p}), \tag{8}$$

where $\mathbf{R}_\mathrm{p} \in SO(3)$. Consequently, the error vector between $\mathbf{p}$ and $\mathbf{p}_\mathrm{p}(\varpi)$ expressed in **P** is given by:

$$\boldsymbol{\varepsilon} = \mathbf{R}_\mathrm{p}^\top(\mathbf{p} - \mathbf{p}_\mathrm{p}(\varpi)), \tag{9}$$

where $\boldsymbol{\varepsilon} = [s, e, h]^\top \in \mathbb{R}^3$ consists of the *along-track error* $s$, the *cross-track error* $e$, and the *vertical-track error* $h$; see Figure 1. The along-track error represents the distance from $\mathbf{p}_\mathrm{p}(\varpi)$ to $\mathbf{p}$ along the $x$-axis of the PATH frame, the cross-track error represents the distance along the $y$-axis, while the vertical-track error represents the distance along the $z$-axis.

By differentiating $\boldsymbol{\varepsilon}$ with respect to time, we obtain:

$$\dot{\boldsymbol{\varepsilon}} = \dot{\mathbf{R}}_\mathrm{p}^\top(\mathbf{p} - \mathbf{p}_\mathrm{p}) + \mathbf{R}_\mathrm{p}^\top(\dot{\mathbf{p}} - \dot{\mathbf{p}}_\mathrm{p}), \tag{10}$$

where:

$$\dot{\mathbf{R}}_\mathrm{p} = \mathbf{R}_\mathrm{p}\mathbf{S}_\mathrm{p} \tag{11}$$

with:

$$\mathbf{S}_\mathrm{p} = \begin{bmatrix} 0 & -\dot{\chi}_\mathrm{p}\cos\upsilon_\mathrm{p} & \dot{\upsilon}_\mathrm{p} \\ \dot{\chi}_\mathrm{p}\cos\upsilon_\mathrm{p} & 0 & \dot{\chi}_\mathrm{p}\sin\upsilon_\mathrm{p} \\ -\dot{\upsilon}_\mathrm{p} & -\dot{\chi}_\mathrm{p}\sin\upsilon_\mathrm{p} & 0 \end{bmatrix}, \quad (12)$$

which is skew-symmetric; $\mathbf{S}_\mathrm{p} = -\mathbf{S}_\mathrm{p}^\top$. We also have that:

$$\dot{\mathbf{p}} = \dot{\mathbf{p}}_\mathrm{dv} = \mathbf{R}_\mathrm{dv}\mathbf{v}_\mathrm{dv}, \quad (13)$$

where $\mathbf{R}_\mathrm{dv} \in SO(3)$ represents a rotation matrix from the INERTIAL frame to a frame attached to the ideal particle with its $x$-axis along the velocity vector of the particle. Let this frame be called the DESIRED VELOCITY frame (**DV**). Hence, the vector $\mathbf{v}_\mathrm{dv} = [U_\mathrm{d}, 0, 0]^\top \in \mathbb{R}^3$ represents the ideal particle velocity with respect to **I**, represented in **DV**. The rotation matrix $\mathbf{R}_\mathrm{dv}$ is selected to be defined by:

$$\mathbf{R}_\mathrm{dv} = \mathbf{R}_\mathrm{p}\mathbf{R}_\mathrm{r}, \quad (14)$$

where:

$$\mathbf{R}_\mathrm{r} = \mathbf{R}_\mathrm{r,z}(\chi_\mathrm{r})\mathbf{R}_\mathrm{r,y}(\upsilon_\mathrm{r}) \quad (15)$$

with $\mathbf{R}_\mathrm{r}$, $\mathbf{R}_\mathrm{r,z}$, and $\mathbf{R}_\mathrm{r,y}$ all elements of $SO(3)$. This way of defining $\mathbf{R}_\mathrm{dv}$ entails that the **DV** frame is obtained by first performing an initial rotation represented by $\mathbf{R}_\mathrm{p}$, resulting in an intermediate frame parallel to the **P** frame, before a relative rotation represented by $\mathbf{R}_\mathrm{r}$ is performed to arrive in **DV**. Obviously, $\mathbf{R}_\mathrm{r}$ (i.e. the angular variables $\chi_\mathrm{r}$ and $\upsilon_\mathrm{r}$) must be designed to ensure that the generalized cross-track error approaches zero (while $\mathbf{R}_\mathrm{r}$ approaches **I**), thus solving the geometric task of the guidance-based path following problem.

Continuing to elaborate on (10), we also have that:

$$\dot{\mathbf{p}}_\mathrm{p} = \mathbf{R}_\mathrm{p}\mathbf{v}_\mathrm{p}, \quad (16)$$

where $\mathbf{v}_\mathrm{p} = [U_\mathrm{p}, 0, 0]^\top \in \mathbb{R}^3$ represents the path particle velocity with respect to **I**, represented in **P**.

By then expanding (10) in light of the recent discussion, we get:

$$\begin{aligned} \dot{\boldsymbol{\varepsilon}} &= (\mathbf{R}_\mathrm{p}\mathbf{S}_\mathrm{p})^\top(\mathbf{p} - \mathbf{p}_\mathrm{p}) + \mathbf{R}_\mathrm{p}^\top(\mathbf{R}_\mathrm{dv}\mathbf{v}_\mathrm{dv} - \mathbf{R}_\mathrm{p}\mathbf{v}_\mathrm{p}) \\ &= \mathbf{S}_\mathrm{p}^\top\boldsymbol{\varepsilon} + \mathbf{R}_\mathrm{r}\mathbf{v}_\mathrm{dv} - \mathbf{v}_\mathrm{p}. \end{aligned} \quad (17)$$

Now define the positive definite and radially unbounded Control Lyapunov Function (CLF):

$$V_{\boldsymbol{\varepsilon}} = \frac{1}{2}\boldsymbol{\varepsilon}^\top\boldsymbol{\varepsilon} = \frac{1}{2}(s^2 + e^2 + h^2), \quad (18)$$

and differentiate it with respect to time along the trajectories of $\boldsymbol{\varepsilon}$ to obtain:

$$\begin{aligned} \dot{V}_{\boldsymbol{\varepsilon}} &= \boldsymbol{\varepsilon}^\top\dot{\boldsymbol{\varepsilon}} \\ &= \boldsymbol{\varepsilon}^\top\left(\mathbf{S}_\mathrm{p}^\top\boldsymbol{\varepsilon} + \mathbf{R}_\mathrm{r}\mathbf{v}_\mathrm{dv} - \mathbf{v}_\mathrm{p}\right) \\ &= \boldsymbol{\varepsilon}^\top\left(\mathbf{R}_\mathrm{r}\mathbf{v}_\mathrm{dv} - \mathbf{v}_\mathrm{p}\right) \end{aligned} \quad (19)$$

since the skew-symmetry of $\mathbf{S}_\mathrm{p}$ leads to $\boldsymbol{\varepsilon}^\top\mathbf{S}_\mathrm{p}^\top\boldsymbol{\varepsilon} = 0$. By further expansion, we get:

$$\dot{V}_{\boldsymbol{\varepsilon}} = s(U_\mathrm{d}\cos\chi_\mathrm{r}\cos\upsilon_\mathrm{r} - U_\mathrm{p}) + eU_\mathrm{d}\sin\chi_\mathrm{r}\cos\upsilon_\mathrm{r} - hU_\mathrm{d}\sin\upsilon_\mathrm{r}, \quad (20)$$

from where we choose $U_\mathrm{p}$ as:

$$U_\mathrm{p} = U_\mathrm{d}\cos\chi_\mathrm{r}\cos\upsilon_\mathrm{r} + \gamma s, \quad (21)$$

where $\gamma > 0$ becomes a constant gain parameter in the guidance law. Since $\varpi$ is the actual path parametrization variable that we control for guidance purposes, we need to obtain a relationship between $\varpi$ and $U_\mathrm{p}$ to be able to implement (21). By using the kinematic relationship given by (16), we get that:

$$\dot{\varpi} = \frac{U_\mathrm{d}\cos\chi_\mathrm{r}\cos\upsilon_\mathrm{r} + \gamma s}{\sqrt{x_\mathrm{p}'^2 + y_\mathrm{p}'^2 + z_\mathrm{p}'^2}}, \quad (22)$$

which is non-singular for all paths satisfying assumption A.1. By choosing $U_\mathrm{p}$ this way, we achieve:

$$\dot{V}_{\boldsymbol{\varepsilon}} = -\gamma s^2 + eU_\mathrm{d}\sin\chi_\mathrm{r}\cos\upsilon_\mathrm{r} - hU_\mathrm{d}\sin\upsilon_\mathrm{r}. \quad (23)$$

An attractive choice for $\chi_\mathrm{r}$ could be the physically motivated:

$$\chi_\mathrm{r}(e) = \arctan\left(-\frac{e}{\triangle_\mathrm{e}}\right), \quad (24)$$

where $\triangle_\mathrm{e}$ becomes a time-varying guidance variable satisfying A.3, and which is utilized to shape the convergence behavior towards the $xz$-plane of **P**. Such a variable is often referred to as a *lookahead distance* in literature dealing with planar path following along straight lines, and the physical interpretation can be derived from Figure 1. Note that other sigmoid shaping functions are also possible candidates for $\chi_\mathrm{r}(e)$, for instance the $\tanh$ function.

The choice for $\upsilon_\mathrm{r}$ could then be:

$$\upsilon_\mathrm{r}(h) = \arctan\left(\frac{h}{\triangle_\mathrm{h}}\right), \quad (25)$$

where $\triangle_\mathrm{h}$ becomes an additional time-varying guidance variable satisfying A.3. It is utilized to shape the convergence behavior towards the $xy$-plane of **P**. Consequently, by utilizing trigonometric relationships from Figure 1, the derivative of the CLF finally becomes:

$$\dot{V}_{\boldsymbol{\varepsilon}} = -\gamma s^2 - U_\mathrm{d}\left[\cos\upsilon_\mathrm{r}\frac{e^2}{\sqrt{e^2 + \triangle_\mathrm{e}^2}} + \frac{h^2}{\sqrt{h^2 + \triangle_\mathrm{h}^2}}\right], \quad (26)$$

which is negative definite under assumptions A.2 and A.3. With a slight abuse of notation, the following proposition can now be stated:

*Proposition 1:* The geometric task is rendered uniformly globally asymptotically and locally exponentially stable (UGAS/ULES) under assumptions A.1-A.3 if $\varpi$ is updated by (22), $\chi_\mathrm{r}$ is equal to (24), and $\upsilon_\mathrm{r}$ is equal to (25).

*Proof:* See [7]. ■

The dynamic task is then fulfilled by assigning a desired speed $U_\mathrm{d}$ which satisfies assumption A.2. In total, we have now solved the ideal spatial guidance-based path following problem.

Since $\triangle_\mathrm{h}$ can be expressed as:

$$\triangle_\mathrm{h} = \mu\sqrt{e^2 + \triangle_\mathrm{e}^2}, \quad (27)$$

where $\mu > 0$, we can rewrite (26) as:

$$\dot{V}_{\boldsymbol{\varepsilon}} = -\gamma s^2 - U_{\mathrm{d}} \left[ \frac{\mu e^2 + h^2}{\sqrt{\mu^2 (e^2 + \triangle_{\mathrm{e}}^2) + h^2}} \right] \tag{28}$$

because:

$$\cos \upsilon_{\mathrm{r}} = \frac{\mu \sqrt{e^2 + \triangle_{\mathrm{e}}^2}}{\sqrt{\mu^2 (e^2 + \triangle_{\mathrm{e}}^2) + h^2}} \tag{29}$$

when expressing $\triangle_{\mathrm{h}}$ as in (27). By choosing the desired speed of the ideal particle as:

$$U_{\mathrm{d}} = \kappa \sqrt{\mu^2 (e^2 + \triangle_{\mathrm{e}}^2) + h^2}, \tag{30}$$

where $\kappa > 0$ is a constant gain parameter, we obtain:

$$\dot{V}_{\boldsymbol{\varepsilon}} = -\gamma s^2 - \mu \kappa e^2 - \kappa h^2, \tag{31}$$

which results in the following proposition:

*Proposition 2:* The geometric task is rendered uniformly globally exponentially stable (UGES) under assumptions A.1 and A.3 if $\varpi$ is updated by (22), $\chi_{\mathrm{r}}$ is equal to (24), $\upsilon_{\mathrm{r}}$ is equal to (25), and $U_{\mathrm{d}}$ satisfies (30).

*Proof:* See [7]. ■

Although very powerful, this result is clearly not achievable by physical systems since these exhibit natural limitations on their maximum attainable speed. In this regard, Proposition 1 states the best possible stability property a spatial vehicle system like an AUV can hold.

We would now like to define an $\mathbf{R}_{\mathrm{dv}}$ that is constructed by only two elementary rotations. This is interesting from a control perspective, especially if we choose not to operate directly in the configuration space. Hence, consider an $\mathbf{R}_{\mathrm{dv}}$ defined by a positive rotation about the $z$-axis of $\mathbf{I}$ by a desired azimuth angle $\chi_{\mathrm{d}}$, followed by a positive rotation about the $y$-axis of the resulting intermediate frame by a desired elevation angle $\upsilon_{\mathrm{d}}$:

$$\mathbf{R}_{\mathrm{dv}} = \mathbf{R}_{\mathrm{dv,z}}(\chi_{\mathrm{d}}) \mathbf{R}_{\mathrm{dv,y}}(\upsilon_{\mathrm{d}}), \tag{32}$$

where $\mathbf{R}_{\mathrm{dv,z}}$ and $\mathbf{R}_{\mathrm{dv,y}}$ both are elements of $SO(3)$. Obviously, the rotations represented by (14) and (32) are not equivalent, i.e. the $y$- and $z$-axes of the two resulting frames are not aligned. However, the rotations map the velocity vector $\mathbf{v}_{\mathrm{dv}}$ equivalently to the INERTIAL frame, which is what matters here. Therefore, by equating the first column (which represents a rotation of the $x$-axis) of (14) with that of (32), we obtain:

$$\chi_{\mathrm{d}} = \arctan \left( \begin{array}{c} \dfrac{\cos\chi_{\mathrm{p}} \sin\chi_{\mathrm{r}} \cos\upsilon_{\mathrm{r}} +}{-\sin\chi_{\mathrm{p}} \sin\chi_{\mathrm{r}} \cos\upsilon_{\mathrm{r}} +} \cdots \\ \dfrac{-\sin\upsilon_{\mathrm{p}} \sin\upsilon_{\mathrm{r}} \sin\chi_{\mathrm{p}} +}{-\sin\upsilon_{\mathrm{p}} \sin\upsilon_{\mathrm{r}} \cos\chi_{\mathrm{p}} +} \cdots \\ \dfrac{\sin\chi_{\mathrm{p}} \cos\chi_{\mathrm{r}} \cos\upsilon_{\mathrm{p}} \cos\upsilon_{\mathrm{r}}}{\cos\chi_{\mathrm{p}} \cos\chi_{\mathrm{r}} \cos\upsilon_{\mathrm{p}} \cos\upsilon_{\mathrm{r}}} \end{array} \right), \tag{33}$$

and

$$\upsilon_{\mathrm{d}} = \arcsin(\sin\upsilon_{\mathrm{p}} \cos\upsilon_{\mathrm{r}} \cos\chi_{\mathrm{r}} + \cos\upsilon_{\mathrm{p}} \sin\upsilon_{\mathrm{r}}), \tag{34}$$

which are the guidance signals that the velocity vector orientation must satisfy in order to ensure geometric path convergence.

## IV. AUV Control Concept

This section presents the control concept that ensures guidance-based path following for an AUV.

### A. Equations of Motion

The 6 degrees-of-freedom (DOFs) kinematics of an AUV can be represented by [8]:

$$\dot{\boldsymbol{\eta}} = \mathbf{J}(\Theta) \boldsymbol{\nu}, \tag{35}$$

where $\boldsymbol{\eta} = [x, y, z, \phi, \theta, \psi]^{\top} \in \mathbb{R}^3 \times \mathcal{S}^3$ (earth-fixed position and attitude), $\Theta = [\phi, \theta, \psi]^{\top} \in \mathcal{S}^3$ (3D torus; three angles defined on $[-\pi, \pi]$), and $\boldsymbol{\nu} = [u, v, w, p, q, r]^{\top} \in \mathbb{R}^6$ (vessel-fixed linear and angular velocities). In what follows, we will also utilize the notation $\mathbf{p} = [x, y, z]^{\top}$, $\mathbf{v} = [u, v, w]^{\top}$, and $\boldsymbol{\omega} = [p, q, r]^{\top}$, all elements of $\mathbb{R}^3$.

Additionally:

$$\mathbf{J}(\Theta) = \begin{bmatrix} \mathbf{R}(\Theta) & \mathbf{0}_{3\times3} \\ \mathbf{0}_{3\times3} & \mathbf{T}(\Theta) \end{bmatrix}, \tag{36}$$

where:

$$\mathbf{R}(\Theta) = \begin{bmatrix} c\psi c\theta & -s\psi c\phi + c\psi s\theta s\phi & s\psi s\phi + c\psi c\phi s\theta \\ s\psi c\theta & c\psi c\phi + s\phi s\theta s\psi & -c\psi s\phi + s\theta s\psi c\phi \\ -s\theta & c\theta s\phi & c\theta c\phi \end{bmatrix} \tag{37}$$

is the rotation matrix from the earth-fixed NED frame (**N**) to the vessel-fixed BODY frame (**B**), parametrized by the three Euler angles in $\Theta$ through three consecutive elementary rotations by the $zyx$-convention. Also:

$$\mathbf{T}(\Theta) = \begin{bmatrix} 1 & s\phi t\theta & c\phi t\theta \\ 0 & c\phi & -s\phi \\ 0 & s\phi / c\theta & c\phi / c\theta \end{bmatrix} \tag{38}$$

relates the vessel-fixed angular velocity vector $\boldsymbol{\omega}$ to $\dot{\Theta}$. For notational brevity, $c\cdot = \cos(\cdot)$, $s\cdot = \sin(\cdot)$, and $t\cdot = \tan(\cdot)$ has been used. At this point, it should be noted that $\mathbf{T}$ is undefined for $\theta = \pm\frac{\pi}{2}$. This is a representational singularity relating to the use of Euler angles for representing the attitude in 3D space (a so-called gimbal lock), and is not kinematically inherent. Such a singularity can be avoided in several ways; by switching between two different Euler angle representations in the vicinity of their singularities, by using a nonsingular four-parameter unit quaternion representation, or by operating directly in the configuration space. However, we will employ the Euler angle $zyx$-convention in this paper due to the intuition associated with it.

The 6 DOF kinetics of an AUV can be represented by [8]:

$$\mathbf{M}\dot{\boldsymbol{\nu}} + \mathbf{C}(\boldsymbol{\nu})\boldsymbol{\nu} + \mathbf{D}(\boldsymbol{\nu})\boldsymbol{\nu} + \mathbf{g}(\Theta) = \boldsymbol{\tau} + \mathbf{J}(\Theta)^{-1}\mathbf{b}, \tag{39}$$

where $\mathbf{M}$ is the vehicle inertia matrix, $\mathbf{C}(\boldsymbol{\nu})$ is the centrifugal and coriolis matrix, $\mathbf{D}(\boldsymbol{\nu})$ is the hydrodynamic damping matrix, and $\mathbf{g}(\Theta)$ represents hydrostatic forces and moments. The system matrices in (39) are assumed to satisfy the properties $\mathbf{M} = \mathbf{M}^{\top} > 0$, $\mathbf{C} = -\mathbf{C}^{\top}$ and $\mathbf{D} > 0$. Furthermore, $\boldsymbol{\tau}$ represents the vessel-fixed propulsion forces and moments, while $\mathbf{b}$ accounts for the earth-fixed low-frequency environmental forces acting on the vehicle.

### B. Control System Design

A nonlinear, model-based velocity and attitude controller is designed by using the backstepping technique. The output-to-be-controlled is redefined from position and attitude to (linear) velocity and attitude. By feeding the controller the appropriate guidance signals, positional convergence is ensured such that the guidance-based path following task objectives are met. This approach resembles the real-life action of a helmsman, who uses vehicle velocity to maneuver. He does not think in terms of directly controlling the position, but in his mind feeds the position error signal back through the velocity assignment, ensuring position control indirectly through direct velocity control. Since such a technique is equally effective for fully actuated and underactuated vehicles, the controller assumes the structure of a velocity and attitude controller.

Start by defining the projection matrix:

$$\mathbf{H} = \begin{bmatrix} \mathbf{0}_{3\times3} & \mathbf{I}_{3\times3} \end{bmatrix}, \tag{40}$$

then the error variables:

$$\begin{aligned} \mathbf{z}_1 &= \Theta - \Theta_{\mathrm{d}} && (41) \\ \mathbf{z}_2 &= \boldsymbol{\nu} - \boldsymbol{\alpha}, && (42) \end{aligned}$$

where $\boldsymbol{\alpha} \in \mathbb{R}^6$ is a vector of stabilizing functions to be specified later.

Define the Control Lyapunov Function (CLF):

$$V_1 = \frac{1}{2}\mathbf{z}_1^\top \mathbf{K}_1 \mathbf{z}_1, \tag{43}$$

where $\mathbf{K}_1 = \mathbf{K}_1^\top > 0$. Differentiating $V_1$ with respect to time along the $\mathbf{z}_1$-dynamics yields:

$$\begin{aligned} \dot{V}_1 &= \mathbf{z}_1^\top \mathbf{K}_1 \dot{\mathbf{z}}_1 \\ &= \mathbf{z}_1^\top \mathbf{K}_1 (\dot{\Theta} - \dot{\Theta}_{\mathrm{d}}) \\ &= \mathbf{z}_1^\top \mathbf{K}_1 (\mathbf{T}\boldsymbol{\omega} - \dot{\Theta}_{\mathrm{d}}), && (44) \end{aligned}$$

since $\dot{\Theta} = \mathbf{T}\boldsymbol{\omega}$. By using (42), we further obtain:

$$\begin{aligned} \dot{V}_1 &= \mathbf{z}_1^\top \mathbf{K}_1 (\mathbf{T}\mathbf{H}(\mathbf{z}_2 + \boldsymbol{\alpha}) - \dot{\Theta}_{\mathrm{d}}) \\ &= \mathbf{z}_1^\top \mathbf{K}_1 \mathbf{T}\mathbf{H}\mathbf{z}_2 + \mathbf{z}_1^\top \mathbf{K}_1 (\mathbf{T}\boldsymbol{\alpha}_{\boldsymbol{\omega}} - \dot{\Theta}_{\mathrm{d}}) && (45) \end{aligned}$$

where $\boldsymbol{\alpha}_{\boldsymbol{\omega}} = \mathbf{H}\boldsymbol{\alpha}$. This motivates the choice of $\boldsymbol{\alpha}_{\boldsymbol{\omega}}$ as:

$$\boldsymbol{\alpha}_{\boldsymbol{\omega}} = \mathbf{T}^{-1}(\dot{\Theta}_{\mathrm{d}} - \mathbf{z}_1), \tag{46}$$

which results in:

$$\dot{V}_1 = -\mathbf{z}_1^\top \mathbf{K}_1 \mathbf{z}_1 + \mathbf{z}_2^\top \mathbf{H}^\top \mathbf{T}^\top \mathbf{K}_1 \mathbf{z}_1. \tag{47}$$

Augment $V_1$ to obtain:

$$V_2 = V_1 + \frac{1}{2}\mathbf{z}_2^\top \mathbf{M}\mathbf{z}_2 + \frac{1}{2}\tilde{\mathbf{b}}^\top \boldsymbol{\Gamma}^{-1}\tilde{\mathbf{b}}, \tag{48}$$

where $\tilde{\mathbf{b}} \in \mathbb{R}^6$ is an adaptation error defined as $\tilde{\mathbf{b}} = \hat{\mathbf{b}} - \mathbf{b}$ with $\hat{\mathbf{b}}$ being the estimate of $\mathbf{b}$, and by assumption $\dot{\mathbf{b}} = \mathbf{0}$. $\boldsymbol{\Gamma} = \boldsymbol{\Gamma}^\top > 0$ is the adaptation gain matrix.

Differentiating $V_2$ along the trajectories of $\mathbf{z}_1$, $\mathbf{z}_2$, and $\tilde{\mathbf{b}}$, we obtain:

$$\dot{V}_2 = -\mathbf{z}_1^\top \mathbf{K}_1 \mathbf{z}_1 + \mathbf{z}_2^\top (\mathbf{H}^\top \mathbf{T}^\top \mathbf{K}_1 \mathbf{z}_1 + \mathbf{M}\dot{\mathbf{z}}_2) + \tilde{\mathbf{b}}^\top \boldsymbol{\Gamma}^{-1}\dot{\hat{\mathbf{b}}}, \tag{49}$$

since $\mathbf{M} = \mathbf{M}^\top$ and $\dot{\tilde{\mathbf{b}}} = \dot{\hat{\mathbf{b}}}$. By rewriting $\mathbf{g}(\Theta) = \mathbf{g}$, $\mathbf{C}(\boldsymbol{\nu}) = \mathbf{C}$, and $\mathbf{D}(\boldsymbol{\nu}) = \mathbf{D}$ from (39) for notational brevity, we have that:

$$\begin{aligned} \mathbf{M}\dot{\mathbf{z}}_2 &= \mathbf{M}(\dot{\boldsymbol{\nu}} - \dot{\boldsymbol{\alpha}}) \\ &= \boldsymbol{\tau} + \mathbf{J}^{-1}\mathbf{b} - \mathbf{g} - \mathbf{D}\boldsymbol{\nu} - \mathbf{C}\boldsymbol{\nu} - \mathbf{M}\dot{\boldsymbol{\alpha}}, && (50) \end{aligned}$$

which yields:

$$\begin{aligned} \dot{V}_2 &= -\mathbf{z}_1^\top \mathbf{K}_1 \mathbf{z}_1 + \mathbf{z}_2^\top (\mathbf{H}^\top \mathbf{T}^\top \mathbf{K}_1 \mathbf{z}_1 + \boldsymbol{\tau} + \mathbf{J}^{-1}\mathbf{b} - \mathbf{g}) + \\ &\quad \mathbf{z}_2^\top (-\mathbf{D}\boldsymbol{\nu} - \mathbf{C}\boldsymbol{\nu} - \mathbf{M}\dot{\boldsymbol{\alpha}}) + \tilde{\mathbf{b}}^\top \boldsymbol{\Gamma}^{-1}\dot{\hat{\mathbf{b}}}. && (51) \end{aligned}$$

Utilizing the fact that $\boldsymbol{\nu} = \mathbf{z}_2 + \boldsymbol{\alpha}$ and $\mathbf{b} = \hat{\mathbf{b}} - \tilde{\mathbf{b}}$, we obtain:

$$\begin{aligned} \dot{V}_2 &= -\mathbf{z}_1^\top \mathbf{K}_1 \mathbf{z}_1 - \mathbf{z}_2^\top \mathbf{D}\mathbf{z}_2 - \mathbf{z}_2^\top \mathbf{C}\mathbf{z}_2 + \\ &\quad \mathbf{z}_2^\top (\mathbf{H}^\top \mathbf{T}^\top \mathbf{K}_1 \mathbf{z}_1 + \boldsymbol{\tau} + \mathbf{J}^{-1}\hat{\mathbf{b}} - \mathbf{g}) + \\ &\quad \mathbf{z}_2^\top (-\mathbf{D}\boldsymbol{\alpha} - \mathbf{C}\boldsymbol{\alpha} - \mathbf{M}\dot{\boldsymbol{\alpha}}) + \\ &\quad \tilde{\mathbf{b}}^\top \boldsymbol{\Gamma}^{-1}(\dot{\hat{\mathbf{b}}} - \boldsymbol{\Gamma}\mathbf{J}^{-\top}\mathbf{z}_2), && (52) \end{aligned}$$

where $\mathbf{z}_2^\top \mathbf{C}\mathbf{z}_2 = 0$ since $\mathbf{C}$ is skew-symmetric [8]. By assigning:

$$\boldsymbol{\tau} = \mathbf{M}\dot{\boldsymbol{\alpha}} + \mathbf{C}\boldsymbol{\alpha} + \mathbf{D}\boldsymbol{\alpha} + \mathbf{g} - \mathbf{J}^{-1}\hat{\mathbf{b}} - \mathbf{H}^\top \mathbf{T}^\top \mathbf{K}_1 \mathbf{z}_1 - \mathbf{K}_2 \mathbf{z}_2, \tag{53}$$

where $\mathbf{K}_2 = \mathbf{K}_2^\top > 0$, and by choosing:

$$\dot{\hat{\mathbf{b}}} = \boldsymbol{\Gamma}\mathbf{J}^{-\top}\mathbf{z}_2, \tag{54}$$

we finally obtain:

$$\dot{V}_2 = -\mathbf{z}_1^\top \mathbf{K}_1 \mathbf{z}_1 - \mathbf{z}_2^\top (\mathbf{D} + \mathbf{K}_2)\mathbf{z}_2. \tag{55}$$

By a slight abuse of notation, regarding the global nature of the stability in question (which strictly is not satisfied due to the representational singularity of the chosen kinematics at $\theta = \pm\frac{\pi}{2}$), we arrive at the following proposition:

*Proposition 3:* For smooth reference trajectories $\mathbf{v}_{\mathrm{d}}, \dot{\mathbf{v}}_{\mathrm{d}} \in \mathcal{L}_\infty$ and $\Theta_{\mathrm{d}}, \dot{\Theta}_{\mathrm{d}}, \ddot{\Theta}_{\mathrm{d}} \in \mathcal{L}_\infty$, the origin of the error system $\left[\mathbf{z}_1^\top, \mathbf{z}_2^\top, \tilde{\mathbf{b}}^\top\right]^\top$ becomes UGAS/ULES by choosing the control and disturbance adaptation laws as in (53) and (54), respectively.

*Proof:* [Indication] The proof can be carried out by utilizing Theorem A.5 from [8]. ■

Please note that this velocity and attitude controller in itself achieves nothing unless it is fed the proper reference signals from a guidance system.

## V. AUV GUIDANCE CONCEPT

We now look at the design of the reference signals required for guiding a controlled AUV such that it meets the guidance-based path following task objectives, and start out by defining $\Theta_{\rm d}$. Since we rely on the guidance laws from Section III to ensure path following, we will utilize the definition of the desired rotation matrix $\mathbf{R}_{\rm dv}$ as given in (32) for the purpose, as we have chosen not to operate directly in the configuration space. This means that we want the velocity vector of the AUV to be oriented in 3D space as given by the Euler angles $\chi_{\rm d}$ and $\upsilon_{\rm d}$. However, the actual velocity vector is oriented in 3D space as given by $\chi$ and $\upsilon$ from (1) and (2), respectively. These Euler angles define the rotation matrix $\mathbf{R}_{\rm v} \in SO(3)$, representing a rotation from **N** to the VELOCITY frame (**V**) by:

$$\mathbf{R}_{\rm v} = \mathbf{R}_{\rm v,z}(\chi)\mathbf{R}_{\rm v,y}(\upsilon), \tag{56}$$

while the rotation matrix $\mathbf{R}_{\rm b} \in SO(3)$, representing a rotation from **N** to **B** have already been defined in (37) by the $zyx$-convention. Consequently, we define the sideslip angle $\beta$ by:

$$\beta = \chi - \psi, \tag{57}$$

and the angle-of-attack $\alpha$ by:

$$\alpha = \upsilon - \theta, \tag{58}$$

deviating from the definitions of $\beta$ and $\alpha$ traditionally found in the hydro- and aerodynamics literature, like [9] and [10]. However, (57) and (58) represent appropriate definitions from a guidance point-of-view, which is of our concern. Consequently, the desired rotation matrix $\mathbf{R}_{\rm db} \in SO(3)$, representing a rotation from **N** to the DESIRED BODY frame (**DB**) is defined by three consecutive elementary rotations (adhering to the $zyx$-convention) by:

$$\mathbf{R}_{\rm db} = \mathbf{R}_{\rm db,z}(\psi_{\rm d})\mathbf{R}_{\rm db,y}(\theta_{\rm d})\mathbf{R}_{\rm db,x}(\phi_{\rm d}) \tag{59}$$

where:

$$\psi_{\rm d} = \chi_{\rm d} - \beta \tag{60}$$

$$\theta_{\rm d} = \upsilon_{\rm d} - \alpha \tag{61}$$

$$\phi_{\rm d} = \phi_{\rm d}, \tag{62}$$

which then constitute $\Theta_{\rm d}$, i.e. $\Theta_{\rm d} = [\phi_{\rm d}, \theta_{\rm d}, \psi_{\rm d}]^\top \in \mathcal{S}^3$. This $\Theta_{\rm d}$ applies regardless of the actuator capability of the AUV in question, and together with $\Theta$ it defines $\boldsymbol{\alpha}_{\boldsymbol{\omega}}$ through (46).

The control vector of a fully actuated AUV is given by:

$$\boldsymbol{\tau}_{\rm f} = [\tau_{\rm X}, \tau_{\rm Y}, \tau_{\rm Z}, \tau_{\rm K}, \tau_{\rm M}, \tau_{\rm N}]^\top, \tag{63}$$

which means that the AUV can independently control all DOFs simultaneously, i.e. independently control the linear velocity and the attitude. Hence, while the velocity vector is required to adhere to the guidance laws from Section III in order to achieve path convergence, the attitude can satisfy some auxiliary task objectives. In this context, define the rotation matrix:

$$\mathbf{R}_{\rm gb} = \mathbf{R}_{\rm gb,z}(\psi_{\rm g})\mathbf{R}_{\rm gb,y}(\theta_{\rm g})\mathbf{R}_{\rm gb,x}(\phi_{\rm g}), \tag{64}$$

representing a rotation from **N** to a GEARED BODY frame (**GB**), $\mathbf{R}_{\rm gb} \in SO(3)$. The **GB** frame represents the reference attitude that only a fully actuated AUV can attain, and $\Theta_{\rm g}$ can be given directly by a human operator or through some high-level guidance system functionality. Note that $\phi_{\rm g} = \phi_{\rm d}$. Since we have that:

$$\mathbf{R}_{\rm gb}\mathbf{v}_{\rm gb} = \mathbf{R}_{\rm dv}\mathbf{v}_{\rm dv}, \tag{65}$$

we get that:

$$\mathbf{v}_{\rm gb} = \mathbf{R}_{\rm gb}^\top\mathbf{R}_{\rm dv}\mathbf{v}_{\rm dv}, \tag{66}$$

which gives us the desired body-fixed linear velocity:

$$\mathbf{v}_{\rm d} = \mathbf{v}_{\rm gb}, \tag{67}$$

which also constitutes $\boldsymbol{\alpha}_{\mathbf{v}}$. Hence, we have that:

$$\boldsymbol{\alpha} = \left[\boldsymbol{\alpha}_{\mathbf{v}}^\top, \boldsymbol{\alpha}_{\boldsymbol{\omega}}^\top\right]^\top \tag{68}$$

Higher order derivatives of $\mathbf{v}_{\rm d}$ and $\Theta_{\rm d}$ can be generated by processing them through a reference model which is adjusted to the closed loop AUV dynamics.

The control vector of the most common type of underactuated AUVs in operation is given by:

$$\boldsymbol{\tau}_{\rm u} = [\tau_{\rm X}, 0, 0, 0, \tau_{\rm M}, \tau_{\rm N}]^\top, \tag{69}$$

which means that only the surge, pitch and yaw DOFs are actuated. In this case, the linear velocity and the attitude of the AUV are inextricably linked together and cannot be independently controlled. This entails that the attitude must be actively used to point the linear velocity vector in the direction requested by the guidance system in order to achieve path convergence. Note that equation (53) can still be kept valid by assigning the required expressions to $\tau_{\rm X}$, $\tau_{\rm M}$ and $\tau_{\rm N}$, while simultaneously imposing dynamics on the stabilizing functions corresponding to the unactuated DOFs such that (53) is satisfied [11]. An analysis of the resulting $\boldsymbol{\alpha}$-subsystem reveals that the stabilizing functions, and hence also the sway, heave and roll speeds, remain bounded. This is an inherent feature of the ambient water-vehicle system due to the fortunate property of hydrodynamic damping.

## VI. UNIFIED CONTROL CONCEPT

Consider a weighting variable $\sigma_{\rm i} \in [0, 1]$ for which:

- $\sigma_{\rm i} = 1$ indicates an actuated DOF,
- $\sigma_{\rm i} = 0$ indicates an unactuated DOF.

Here, $i \in \mathcal{U} = [Y, Z, K]$, where $\mathcal{U}$ is the index set representing the AUV DOFs rendered uncontrollable at high speeds. The $\sigma_{\rm i}$ variables could be implemented as sigmoid functions, ensuring a smooth transition between the actuated and unactuated case. A natural choice would be to make them depend on the instantaneous AUV speed, i.e. $\sigma_{\rm i} = \sigma_{\rm i}(U)$.

Now, consider a DOF with a transitional speed zone between actuation and unactuation represented by a lower limit of $U_{\mathrm{f,i}}$ corresponding to actuation, and an upper limit of $U_{\mathrm{u,i}}$ corresponding to unactuation. Then the choice of $\sigma_{\mathrm{i}}$ could be:

$$\sigma_{\mathrm{i}}(U) = 1 - \frac{1}{2}\left(\tanh\left(\frac{U - \frac{U_{\mathrm{f,i}}+U_{\mathrm{u,i}}}{2}}{\triangle_{\sigma,\mathrm{i}}}\right) + 1\right), \quad (70)$$

where $U = \sqrt{u^2+v^2+w^2} \geq 0$ is the vehicle speed, and $\triangle_{\sigma,\mathrm{i}} > 0$ shapes the steepness of the transitional speed zone. By denoting the relevant control input for an actuated DOF as $\tau_{\mathrm{f,i}}$ and for an unactuated DOF as $\tau_{\mathrm{u,i}}$ $(= 0)$, the actual control input enforced at any time can be represented by:

$$\tau_{\mathrm{i}} = \sigma_{\mathrm{i}}\tau_{\mathrm{f,i}} + (1-\sigma_{\mathrm{i}})\tau_{\mathrm{u,i}}. \quad (71)$$

Likewise, the actual stabilizing function can be represented by:

$$\alpha_{\mathrm{i}} = \sigma_{\mathrm{i}}\alpha_{\mathrm{f,i}} + (1-\sigma_{\mathrm{i}})\alpha_{\mathrm{u,i}}, \quad (72)$$

where the stabilizing function for an actuated DOF is given by $\alpha_{\mathrm{f,i}}$ and for an unactuated DOF by $\alpha_{\mathrm{u,i}}$. The former is taken from (68), while the latter is calculated from the associated dynamics of (53).

Summing up, the proposed velocity and attitude controller relies upon the guidance-based path following approach to guarantee positional convergence to any regularly parametrized geometric path in 3D, while the speed-weighted control inputs (71) and stabilizing functions (72) are crucial for the validity of (53) and (54), i.e. that the controller structure is equally effective for both fully actuated and underactuated AUVs, seamlessly across the entire speed regime.

## VII. Case Study: Underactuated AUV in Flight

A simulation is performed with an AUV undertaking a helical flight maneuver. The vehicle data is taken from the NPS AUV II, a slender-body AUV with a mass of $m = 5454.54\ kg$ and a length of $L = 5.3\ m$ [12]. The AUV is exposed to a constant environmental force during the run. Since the AUV operates at $1.5\ m/s$ during the maneuver, it represents an underactuated AUV unactuated in the sway, heave, and roll DOFs. The initial vehicle states are $\boldsymbol{\eta}_0 = [-25, 0, 0, 0, 0.17, 0.44]^\top$ (units $[m]/[rad]$), and $\boldsymbol{\nu}_0 = [1.5, 0, 0, 0, 0, 0]^\top$ (units $[m/s]/[rad/s]$). The guidance parameter is fixed at $\gamma = 100$, while the guidance variables are chosen by $\triangle_{\mathrm{e}} = 2L$ and $\mu = 1$. The controller and adaptation gains are chosen as $\mathbf{K}_1 = \mathbf{K}_2 = 10^3\mathbf{I}$, and $\boldsymbol{\Gamma} = 10^2\mathbf{I}$, respectively. Figure 2 shows that the AUV converges elegantly to the path while behaving as a weathervane; pointing towards the environmental disturbance.

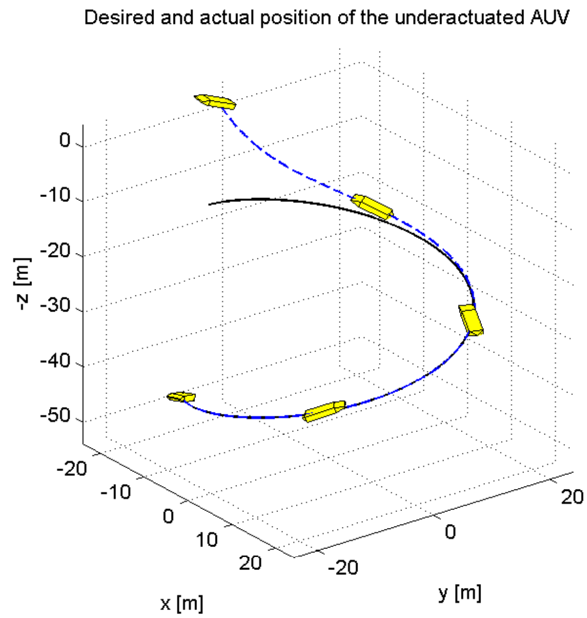


Fig. 2. The underactuated AUV converges naturally to the desired path.

## VIII. Conclusions

A single controller structure has been proposed for the automatic control of AUVs through their non-zero speed envelope. The design is made possible by a nonlinear, model-based velocity and attitude controller relying on a guidance-based path following concept necessary to ensure geometric path convergence. It guarantees that a vehicle which is fully actuated at low speeds, but becomes underactuated at high speeds, is able to converge to and follow a desired geometric path independent of its speed.

## References


[1] J. S. Riedel and A. J. Healey, "Shallow water station keeping of AUVs using multi-sensor fusion for wave disturbance prediction and compensation," in *Proceedings of the OCEANS'98, Nice, France*, 1998.

[2] K. D. Do and J. Pan, "Robust and adaptive path following for underactuated autonomous underwater vehicles," in *Proceedings of the ACC'03, Denver, Colorado, USA*, 2003.

[3] D. Bertin and L. Branca, "Operational and design aspects of a precision minewarfare autopilot," in *Proceedings of the Warship 2000, London, UK*, 2000.

[4] M. Breivik and T. I. Fossen, "A unified concept for controlling a marine surface vessel through the entire speed envelope," in *Proceedings of the MED'05, Limassol, Cyprus*, 2005.

[5] ——, "Guidance-based path following for autonomous underwater vehicles," in *Proceedings of the OCEANS'05, Washington D.C., USA*, 2005.

[6] R. Skjetne, "The maneuvering problem," Ph.D. dissertation, Norwegian University of Science and Technology, Trondheim, Norway, 2005.

[7] M. Breivik and T. I. Fossen, "Principles of guidance-based path following in 2D and 3D," in *Proceedings of the 44th IEEE CDC, Seville, Spain*, 2005.

[8] T. I. Fossen, *Marine Control Systems: Guidance, Navigation and Control of Ships, Rigs and Underwater Vehicles*, 1st ed. Marine Cybernetics, Trondheim, Norway, 2002.

[9] The Society of Naval Architects and Marine Engineers, "Nomenclature for treating the motion of a submerged body through a fluid," 1950, Technical and Research Bulletin No. 1-5.

[10] B. Stevens and F. Lewis, *Aircraft Control and Simulation*, 2nd ed. John Wiley & Sons Inc., 2003.

[11] T. I. Fossen, M. Breivik, and R. Skjetne, "Line-of-sight path following of underactuated marine craft," in *Proceedings of the 6th IFAC MCMC, Girona, Spain*, 2003.

[12] A. J. Healey and D. Lienard, "Multivariable sliding-mode control for autonomous diving and steering of unmanned underwater vehicles," *IEEE Journal of Oceanic Engineering*, vol. 18, no. 3, pp. 327–339, 1993.